Track-Before-Detect for Automotive Multi-Radar Systems with Time-Varying Fields of View

Qing Miao, Zhiyuan Zou, Wujun Li, and Wei Yi
School of Information and Communication Engineering
University of Electronic Science and Technology of China, Chengdu, China
Email: MiaoQing313@163.com, zhiyuan_zou417@163.com, 1224liwujun@gmail.com, kussoyi@gmail.com

***Abstract*—Track-before-detect (TBD) and multi-sensor fusion are two popular methods of weak target detection which can improve the performance by increasing the number of measurements. In this paper, we combine these two methods, proposing a novel multi-sensor track-before-detect (MS-TBD) method for automotive platforms. It can utilize the information from both the spatial and temporal dimensions of the target by jointly processing the measurement from different radars. In particular, the traditional TBD method is often based on an implicit assumption: the presence of targets is unchanged in the sliding window. However, this assumption may not be applicable for automotive multi-sensor systems due to the time-varying fields of view (FOV). To solve the problems mentioned above, we first present an energy accumulation strategy for automotive multi-radar systems and then propose a multiple-hypothesis detection method with the adaptive threshold (AT). It is demonstrated by simulations that the proposed methods show superior performance.**

***Index Terms*—Multi-sensor fusion, time-varying field of view, adaptive threshold, TBD method**

I. Introduction

In recent years, with the development of advanced driver assistance systems (ADAS), vehicles need to accurately perceive and understand their surroundings to make safe and intelligent decisions promptly. However, a single radar may have some limitations, such as occlusion, blind spots, or the appearance of false targets [1]. Therefore, multi-sensor fusion (MSF) emerges as a compelling choice, which could achieve a more comprehensive and accurate awareness of the surroundings [2], to assist intelligent driving vehicles in planning paths and accurately avoiding obstacles.

Multi-sensor fusion is a technique that integrates measurements received from multiple sensors, which could acquire the target space-diversity gain by jointly processing the measurement samples on different observation orientations. Naturally, MSF has gained significant attention, with numerous algorithms proposed in this field [3]–[5]. However, most of them mainly focus on single-frame detection (SFD), which involves a thresholding operation on each measurement frame, and only the surviving measurements can be provided to a subsequent tracker [6]. Since the information reduction after thresholding is irreversible, these methods show some limitations, especially for low signal-to-noise ratio (SNR) targets.

This work was supported in part by the National Natural Science Foundation of China under Grant 62231008 and 62301127, in part by the China Postdoctoral Science Foundation under Grant BX20220057, 2023M730509 and GZB20230112, the "Tianfu Qingcheng" Plan of Sichuan Province under Grant1332 and 1395.

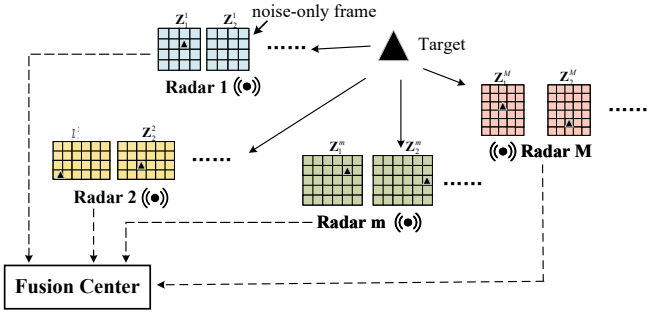

Fig. 1. An illustration of the multi-radar system.

Conversely, multi-frame track-before-detect (MF-TBD) is an effective approach to track weak targets. It could take advantage of the target temporal correlation by jointly processing several consecutive scans to accumulate the target energy and finally enhance the target SNR [7]. In order to apply MF-TBD to practical engineering, it has been studied extensively and proven to be effective in various areas, such as radars [8], [9], optical images [10], and sonars systems [11], [12].

However, when considering the application of the MF-TBD to automotive multi-sensor systems, the alignment of measurements from different frames encounters two inherent limitations. On the one hand, the radar data units (called frames) of multiple radar nodes have different sizes and numbers. On the other hand, the field of view (FOV) of an automotive radar varies over time due to the ego-motion of the vehicle. A multi-station MF-TBD algorithm with a distributed processing architecture is proposed in [13], which first performs MF-TBD at each local radar node to obtain the target track and then fuses the detected track at the fusion center. Nevertheless, this method does not consider the discretization strategy of the state space and the relationship between the scanning area and the state space.

Furthermore, the traditional MF-TBD algorithm is usually based on an implicit assumption in the derivation of the detection threshold: the presence of the target is constant within each sliding window, i.e., each target remains present (or absent) over the entire timeframe corresponding to the current sliding window [14]. However, this assumption may

not always be applicable in the automotive multi-radar system, because the platform is constantly moving, and the observation regions of different radar nodes exhibit variations. As a result, the integration of the multiple frames in the sliding window can not sufficiently accumulate the target energy, resulting in significant performance degradation.

In this paper, we introduce a novel multi-radar fusion strategy for automotive platforms to improve detection performance, which could solve the problem of measurement misalignment caused by the radars' spatial distribution and vehicle movement. The major contributions of this paper are summarized as follows:

• *A energy accumulation strategy for automotive multi-radar systems*: To implement target energy accumulation of multi-frame measurements from different radars in the fusion center, we proposed a motion compensation strategy to build a correspondence of measurement between consecutive frames. It could directly integrate the merit functions in the antenna coordinate systems corresponding to different radars at different frames.

• *A novel multi-sensor track-before-detect method*: Based on the accumulation strategy mentioned above, we develop an adaptable detection threshold-based MS-TBD strategy (AT-MS-TBD). It can adaptively adjust the detection threshold according to the number of frames that effectively accumulate the target energy. Finally, the estimation accuracy of AT-MS-TBD is demonstrated with extensive simulations.

II. Models And Systems

A. Target Model

In this paper, we consider a point target moving in the navigation coordinate system. At the *k*-th frame, the target state is recorded as:

$$\mathbf{x}_k = [x_k^{tar}, \dot{x}_k^{tar}, y_k^{tar}, \dot{y}_k^{tar}]^\top \in \mathbb{R}^4, \tag{1}$$

with $[x_k^{tar}, y_k^{tar}]$ the position and $[\dot{x}_k^{tar}, \dot{y}_k^{tar}]$ the velocity, and $\mathbb{R}^4$ denotes a 4-dimensional space that contains all of the possible target states.

The target motion is usually assumed to satisfy the first-order Markov process, and then the process of changes in the target state over discrete time can be modeled as:

$$\mathbf{x}_{k+1} | \mathbf{x}_k \sim \mathcal{N}(\cdot; \mathbf{F}\mathbf{x}_k, \mathbf{Q}), \tag{2}$$

where $\mathcal{N}(\cdot; \boldsymbol{\mu}, \boldsymbol{\Sigma})$ follows the Gaussian distribution whose mean value is $\boldsymbol{\mu}$ and covariance is $\boldsymbol{\Sigma}$.

To facilitate the description of the algorithm, this paper uses the constant velocity (CV) model as an example. Therefore, the target's state-transition matrix $\mathbf{F}$ and process noise variance matrix $\mathbf{Q}$ in (2) can respectively be expressed as:

$$\mathbf{F} = \begin{bmatrix} 1 & T \\ 0 & 1 \end{bmatrix} \otimes \mathbf{I}_2, \qquad \mathbf{Q} = q_s \cdot \begin{bmatrix} T^3/3 & T^2/2 \\ T^2/2 & T \end{bmatrix} \otimes \mathbf{I}_2, \tag{3}$$

where T is the time between consecutive frames, $\otimes$ is the Kronecker product, and q_s donates a parameter that measures the process noise.

Then, the target state sequence from the first frame to the K-th frame can be expressed as:

$$\boldsymbol{X}_{1:K} = \{\mathbf{x}_1, \mathbf{x}_2, \ldots, \mathbf{x}_K\}. \tag{4}$$

B. Automotive Multi-radar Systems

It is well known that the global navigation satellite system (GNSS) and inertial measurement unit (IMU) of the ADAS system could provide highly accurate measurements [15], recording the vehicle's location, velocity, and yaw. Then, the vehicle body's state is given by:

$$\Psi_k = [n_k^{car}, \dot{n}_k^{car}, w_k^{car}, \dot{w}_k^{car}, \alpha_k], \tag{5}$$

where α_k is the yaw angle, $[n_k^{car}, w_k^{car}]$ and $[\dot{n}_k^{car}, \dot{w}_k^{car}]$ are respectively the position and the speed of the vehicle in the navigation coordinate system.

We assume that the automotive multi-radar system consists of M independent radars and a fusion center. The state of the *m*-th radar relative to the vehicle body is expressed as:

$$\mathbf{S}^m = (f^m, l^m, \beta^m), \tag{6}$$

where f^m and l^m are respectively the forward and left positions of the *m*-th radar relative to the center of the vehicle body, and β^m is the installation angle.

The raw measurements obtained from the *m*-th radar will be transmitted to the fusion center and converted into discrete measurements with N_r^m range cells, $N_{\dot{r}}^m$ Doppler cells, N_θ^m azimuth cells, and $N_{\dot{\theta}}^m$ azimuth velocity.

Therefore, the measurement at the *k*-th frame can be represented as a $N_r^m \times N_{\dot{r}}^m \times N_\theta^m \times N_{\dot{\theta}}^m$ matrix:

$$\begin{aligned} \mathbf{z}_k^m = \{ z_k^m(i,j,n,l) : i \in [1, N_r^m], j \in [1, N_{\dot{r}}^m], \\ n \in [1, N_\theta^m], l \in [1, N_{\dot{\theta}}^m] \}. \end{aligned} \tag{7}$$

After that, the measurement of each cell is modeled as:

$$z_k^m(i,j,n,l) = \begin{cases} |A_k^m + c_k^m(i,j,n,l)| & \text{if target is in } (i,j,n,l) \\ |c_k^m(i,j,n,l)| & \text{otherwise} \end{cases} \tag{8}$$

where A_k^m is the target amplitude received by the *m*-th radar at the *k*-th frame, and $c_k^m(i,j,n,l)$ is the background noise modeled by Gaussian distribution [16]. Then the fusion center receives the measurements $\mathbf{z}_k^m$ and records their sampling time $\mathbf{t}_k^m$, where $m = 1, \cdots, M$, $k = 1, \cdots, K$.

III. Background and Problem Statement

In this section, we first briefly review the traditional TBD, followed by the background and basic assumptions. Then, two challenges of TBD for automotive multi-radar systems are demonstrated.

A. Review of Traditional TBD

TBD conducts a comprehensive search over all feasible paths, and the target is declared once the maximum cumulative

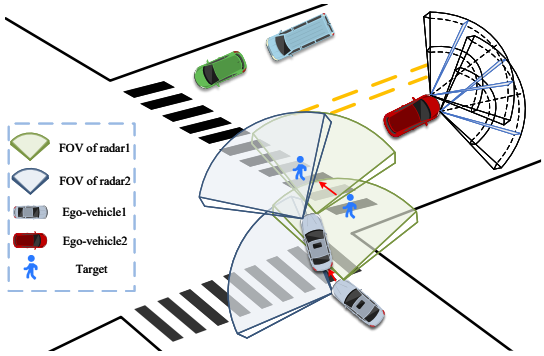

Fig. 2. This is the traffic flow of autonomous vehicles. The figure shows the time-varing FOVs of two consecutive frames in the automotive muti-radar systems. It is seen that: (1) The measurement area is constantly changing due to the movement of ego-vehicle1. (2) The mismatch of demarcation and discretization criterion between different radars on ego-vehicle2. (3) The target only fell into one of the radars measurement area of ego-vehicle1 in the (k-1)-th frame.

energy exceeds the threshold [17]. The expression of TBD for a single target is given as:

$$\begin{aligned} \hat{\mathbf{X}}_{1:K} &= \arg \max_{\mathbf{X}_{1:K} \in \mathbb{R}} p(\mathbf{X}_{1:K} | \mathbf{Z}), \\ s.t. \max_{\mathbf{X}_{1:K} \in \mathbb{R}} p(\mathbf{X}_{1:K} | \mathbf{Z}) &\underset{H_0}{\overset{H_1}{\lessgtr}} V_{DT} \ , \end{aligned} \tag{9}$$

where V_{DT} donates the detection threshold. The target state sequence is written as $\mathbf{X}_{1:K} = [\mathbf{x}_1, \mathbf{x}_2, \cdots, \mathbf{x}_K]$. The target trajectory is successfully declared when the posterior probability $p(\mathbf{X}_{1:K}|\mathbf{Z})$ exceeds the detection threshold V_{DT}.

It is evident that the maximization in (9) is hard to obtained due to the infinity and continuity of state space. Therefore, it is essential to finite and discrete the state space [18], [19]. Then, two preconditions of traditional TBD are outlined as follows:

• For a single ground-based radar, the target's state space is demarcated by the FOV and discretized according to the criterion of discrete measurements, depending on the invariance of the radar's scanning area.

• The traditional TBD algorithm only accumulates energy in the radar's measurement area, and it is usually based on constant presence assumption, i.e., the status of target presence is unchanged within each sliding window.

B. Challenges

1) Mismatch of discrete measurement: According to the Bayes formula, the posterior probability of the target in multi-sensor systems can be expanded as [15]:

$$p(\mathbf{X}_{1:K_M} | \mathbf{Z}) \propto \prod_{k=1}^{K_M} p(\mathbf{z}_k^m | \mathbf{x}_k) \, p(\mathbf{x}_k | \mathbf{x}_{k-1}) \, . \tag{10}$$

where $p(\mathbf{z}_k^m | \mathbf{x}_k)$ describes the relationship between the target state $\mathbf{x}_k$ and the measurement $\mathbf{z}_k^m$.

So we need to establish a correspondence between the state and measurement, because discrete cells of measurements no longer match each other in different frames. On the one hand, the movement of the vehicle results in the misalignment of measurement data obtained at different moments. On the other hand, the different locations of radar nodes introduce spatial misalignment among measurements obtained from different radars at the same moment [20].

When we jointly consider multiple sampling samples in different time dimensions and spatial locations, it becomes a significant challenge to accumulate the target energy directly. Furthermore, affected by the operating mode and system parameters, the number and size of measurement cells, and their position relative to the target vary from one radar to another.

2) Inconsistence of observed target information: In automotive radar systems, vehicles often perform sudden and drastic maneuvers such as U-turns or lane changes. Due to the varying installation locations of the radar and the target motion characteristics, it is not guaranteed that each radar within the system can illuminate the target in each scanning cycle. Consequently, the target may not be within the scanning area for a single frame or several frames, leading to insufficient accumulation of target energy in the sliding window integration process [21]. This ultimately results in a high rate of missed detections and compromises the performance of the algorithm.

IV. The Proposed AT-MS-TBD Algorithm

In response to the two challenges mentioned above, this section introduces a motion compensation strategy for automotive multi-radar systems. Subsequently, we illustrate the core concept and detailed steps of the AT-MS-TBD algorithm.

A. Motion Compensation Strategy for Multi-Sensor Systems

To effectively accumulate target energy from multi-frame measurements originating from different radars in the fusion center, it is imperative to address the challenges posed by the moving platform and the distribution of radar positions. Therefore, we propose a motion compensation strategy that involves compensating for the positions of both the radar and the vehicle. This compensation enables us to establish a correspondence between measurements across consecutive frames, thereby overcoming the above challenges.

In the fusion center, the measurements from different radars are sorted according to the sampling time, where the measurement of the k-th frame can be expressed as

$$\mathbf{Z}_{cen} = \{\mathbf{z}_{cen}^1, \mathbf{z}_{cen}^2, \cdots, \mathbf{z}_{cen}^K\}, \quad K = \sum_{m=1}^{M} K_m. \tag{11}$$

We take one of the cells $[r, \dot{r}, \theta, \dot{\theta}]$ in the k-th frame as an example to describe the process of the motion compensation and valid state transition center searching.

The cell of the gridded state in the antenna coordinate system is first transformed to the vehicle body system by compensating the position and installation angle of the radar where the k-th frame measurement is located:

$$\begin{aligned}\mathbf{C}_k &= [x_k^{veh}, \dot{x}_k^{veh}, y_k^{veh}, \dot{y}_k^{veh}] \\ &= \mathbf{R}(\beta) \cdot \begin{bmatrix} r_k \cos\theta_k \\ \dot{r}_k \cos\theta_k - r_k\dot{\theta}_k \sin\theta_k \\ r_k \sin\theta_k \\ \dot{r}_k \sin\theta_k - r_k\dot{\theta}_k \cos\theta_k \end{bmatrix} + \begin{bmatrix} f_{\varepsilon_k} \\ 0 \\ l_{\varepsilon_k} \\ 0 \end{bmatrix}. \end{aligned} \tag{12}$$

The rotation matrix $\mathbf{R}(\beta)$ could be given by:

$$\mathbf{R}(\beta) = \begin{bmatrix} \cos\beta & 0 & -\sin\beta & 0 \\ 0 & \cos\beta & 0 & -\sin\beta \\ \sin\beta & 0 & \cos\beta & 0 \\ 0 & \sin\beta & 0 & \cos\beta \end{bmatrix}. \tag{13}$$

By compensating the yaw angle a_k and position of the vehicle body $[n_{t_k}^{car}, \dot{n}_{t_k}^{car}, w_{t_k}^{car}, \dot{w}_{t_k}^{car}]$, the state could be transformed into the navigation coordinate system, where we can build the state transition relationship directly:

$$\begin{aligned}\mathbf{S}_k &= [n_k^{nav}, \dot{n}_k^{nav}, w_k^{nav}, \dot{w}_k^{nav}] \\ &= R(\alpha_k) \cdot \mathbf{C}_k + [n_{t_k}^{car}, \dot{n}_{t_k}^{car}, w_{t_k}^{car}, \dot{w}_{t_k}^{car}].\end{aligned} \tag{14}$$

The state of the current cell in the navigation coordinate system at the (k+1)-th is frame based on the target motion model and the interval of consecutive frames $\Delta t = t_{k+1} - t_k$. It can be obtained by:

$$\mathbf{S}_{k+1} = \mathbf{S}_k + \Delta t \cdot [\dot{x}_k^{tar}, 0, \dot{y}_k^{tar}, 0]. \tag{15}$$

To prepare for the energy accumulation, we need to find out where the state $\mathbf{S}_{k+1}$ corresponds to the antenna coordinate system of the radar. The state in the vehicle body system can be obtained by compensating the information of the car at the (k+1)-th frame:

$$\mathbf{C}_k^{k+1} = \left(\mathbf{P}_{k+1} - \mathbf{x}_{t_{k+1}}^{car}\right) \cdot \mathbf{R}^{-1}(\alpha_{k+1}), \tag{16}$$

$$\mathbf{x}_{t_{k+1}}^{car} = \left[n_{t_{k+1}}^{car}, \dot{n}_{t_{k+1}}^{car}, w_{t_{k+1}}^{car}, \dot{w}_{t_{k+1}}^{car}\right]^\top \tag{17}$$

where "-1" indicates the inverse of a matrix.

Then we transform $\mathbf{C}_k^{k+1}$ into the antenna Cartesian coordinate system by compensating for the radar's position and installation angle:

$$\mathbf{x}_k^{k+1} = \mathbf{R}^{-1}(\beta_{\varepsilon_k}) \cdot \left(\mathbf{C}_k^{k+1} - \left[f_{\varepsilon_{k+1}}, 0, l_{\varepsilon_{k+1}}, 0\right]^\top\right). \tag{18}$$

The center cell index of valid state transition space k-th frame can be obtained by:

$$\begin{cases} r_k^{k+1} = \left\lceil \left\| x_k^{k+1}, y_k^{k+1} \right\|_2 / \Delta r \right\rceil \\ \dot{r}_k^{k+1} = \left\lceil (x_k^{k+1}\dot{x}_k^{k+1} + y_k^{k+1}\dot{y}_k^{k+1}) / \left\| x_k^{k+1}, y_k^{k+1} \right\|_2 \right\rceil \\ \theta_k^{k+1} = \left\lceil \arccos\left(y_k^{k+1}/x_k^{k+1}\right) / \Delta\theta \right\rceil \\ \dot{\theta}_k^{k+1} = \left\lceil \left(x_k^{k+1}\dot{y}_k^{k+1} + y_k^{k+1}\dot{x}_k^{k+1}\right) / \left\| x_k^{k+1}, y_k^{k+1} \right\|_2^2 \right\rceil \end{cases}. \tag{19}$$

Remark 1: Our approach also remains applicable to synchronous situations. When the time interval between two consecutive frames is zero, it implies that the target states in these adjacent frames are essentially identical. Consequently, during the integration of merit functions, there is no need to search for a valid state transition space. Instead, we can directly accumulate the measurement to simplify the process and enhance its efficiency.

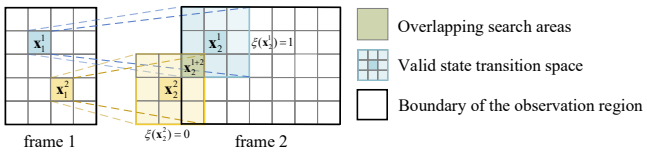

Fig. 3. Schematic diagram of searching for valid state transition space and integrating the merit functions.

B. AT-MS-MFD

Aiming at the problem that the measurements of some frames don't include the target, which affects the full accumulation of target energy, we propose the AT-MS-TBD algorithm in this subsection. It could algorithm adaptively adjust the detection threshold based on the number of frames effectively accumulating target energy.

In the fusion center, we process all measurements using a sliding window approach with the batch length of K. Since the processing is the same in each sliding window, we will use the one as an illustrative example to outline the detailed steps.

1) Initialization

Firstly, we initialize the merit functions of all discrete states $\mathbf{x}_1 = [r_1, \dot{r}_1, \theta_1, \dot{\theta}_1] \in \mathbb{R}$ with the measurement $\mathbf{z}_1$ at the first frame:

$$I_1(\mathbf{x}_1 \,|\mathbf{Z}) = \mathbf{z}_1 \tag{20}$$

$$\Psi_1(\mathbf{x}_1) = 0\ , \tag{21}$$

where $I_1(\mathbf{x}_1 \,|\mathbf{Z})$ denotes the merit function of the $\mathbf{x}_1$, and $\Psi_k(\cdot)$ is used to store state transitions between consecutive frames.

2) Merit Function Integration

As can be seen in Fig. 3, unlike the traditional TBD methods searching for station transition space just within the measurement area, AT-MS-TBD updates the value function for all states $\mathbf{x}_k$ in the $\mathbb{Q}_k = \{\mathbf{x}_k \,|I_k(\mathbf{x}_k) \neq \text{empty}\}$.

However, each cell may be searched not only once, as the green cell $\mathbf{x}_2^{1+2}$ shown in Fig. 3. So we update the merit function $I(\mathbf{x}_2^{1+2})$ based on the larger of $I(\mathbf{x}_1^1)$ and $I(\mathbf{x}_1^2)$. This process can be expressed as:

$$\begin{aligned} I_{k+1}(\mathbf{x}_k^{k+1}) &= \max_{\mathbf{x}_k \in \tau(\mathbf{x}_k^{k+1})} I_k(\mathbf{x}_k) + \left|\mathbf{z}_{k+1}(\mathbf{x}_k^{k+1})\right| \\ \Psi_{k+1}(\mathbf{x}_k^{k+1}) &= \arg \max_{\mathbf{x}_k \in \tau(\mathbf{x}_k^{k+1})} I_k(\mathbf{x}_k), \end{aligned} \tag{22}$$

where $\tau(\mathbf{x}_k^{k+1})$ is the range of states in which the target state may be transferred from the k-th frame.

3) State Cell Labeling:

In the process of accumulating merit functions, we set the parameter ξ_k to mark whether the searched state cell $\mathbf{x}_k$ is located in the measurement area in the k-th frame:

$$\xi_k(\mathbf{x}_k) = \begin{cases} 1, & \text{if } \mathbf{z}_k(i_k, j_k, n_k, l_k) \neq \emptyset \\ 0, & \text{otherwise} \end{cases} . \tag{23}$$

Then, the algorithm can subsequently judge the number of frames that have effectively accumulated to the target energy based on the $\xi_k(\mathbf{x}_k)$ of each frame

$$\varepsilon = \sum_{k=1}^{K} \xi_k(\hat{\mathbf{x}}_k) \ . \tag{24}$$

4) Adaptive Detection and Trajectory Backtracking:

According to this, we can adaptively set thresholds in order to prevent missed detection or false alarms resulting from the absence of a target in some frames. And the uncertainty of the ε will lead to multiple nested assumptions of H_1, i.e., $\{H_{1,\varepsilon}, \varepsilon = 1, ..., K\}$:

$$\hat{\mathbf{x}}_K = \arg \max_{\mathbf{x}_K \in \mathbb{Q}_K} I_K(\mathbf{x}_K) \tag{25}$$

$$s.t. \max_{\mathbf{x}_K \in \mathbb{Q}_K} I_K(\hat{\mathbf{x}}_K) \begin{cases} \underset{H_0}{\overset{H_{1,1}}{\lessgtr}} V_{DT1} \ , & \text{if } \varepsilon = 1 \\ \vdots & \vdots \\ \underset{H_0}{\overset{H_{1,K}}{\lessgtr}} V_{DTK} \ , & \text{if } \varepsilon = K \end{cases} . \tag{26}$$

Finally, the algorithm will backtrack the trajectory. For $k = K-1, \cdots, 1$:

$$\hat{\mathbf{x}}_k = \Psi_{k+1}(\mathbf{x}_{k+1}). \tag{27}$$

Through the AT-MS-TBD algorithm, we can jointly process the measurements from multiple radars in the fusion center to estimate the optimal target state $\hat{\mathbf{X}}_{1:K} = [\hat{\mathbf{x}}_1, \hat{\mathbf{x}}_2, \cdots, \hat{\mathbf{x}}_K]$, even if the target existence is inconsistent.

V. Simulation Examples

In this section, we will verify the performance of the proposed AT-MS-TBD method with Monte Carlo simulations under a given false alarm probability. The probability of efficient target detection (Pd) and root mean square error (RMSE) are used as the quantitative comparison parameters.

We first set up two simple scenarios: two automotive radars detect a single target while maintaining a constant velocity (1m/s, 2m/s). One of the scenarios uses synchronous data, and the other uses asynchronous data. Then, we design a more complex scenario to verify the robustness of the algorithm: the simultaneous presence of synchronous and asynchronous situations, as well as inconsistent target existence between frames. The specific simulation details are as follows:

1) Scenario 1

As can be seen in Fig. 4 (a), we first consider the situation where the measurements of two automotive radars are asynchronous. The two corner radars move with the vehicle body but sample and transmit measurements to the fusion center

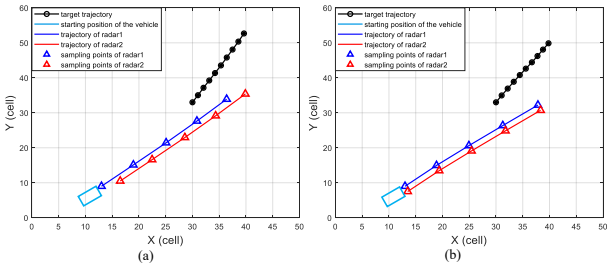

Fig. 4. Schematic diagram of the simulation scenario. (a) Scenario1: asynchronous situation. (b) Scenario2: synchronized situation.

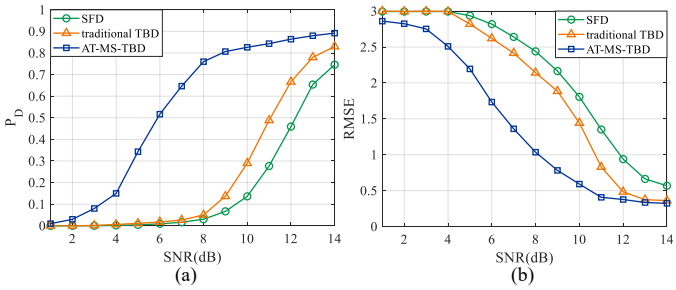

Fig. 5. Scenario 1: The Pd and RMSE curves of three algorithms are plotted against target SNR.

at different moments, respectively. The Pd and RMSE curves are plotted against the SNR to demonstrate the effectiveness of the proposed algorithm, which is compared with the detection performance of a single radar and benchmarked against the traditional SFD method.

The simulation results illustrate that when the two radars work in asynchronous mode, more measurement frames can be collected in the same period for the TBD algorithm to accumulate the target energy. Consequently, we can set the length of the sliding window K=10. As illustrated in Fig. 5, compared with the single-radar MFD, AT-MS-TBD provides a more accurate estimation of all SNR.

2) Scenario 2

Consider a scenario where measurements from two automotive radars are synchronous, as shown in Fig. 4 (b). In the centralized processing approach, the synchronous measurement can be regarded as a particular case of asynchronous measurements, where the time interval between consecutive frames is zero. In such instances, the target state remains entirely consistent between consecutive frames.

During the accumulation of merit functions, we can accumulate the measurements in the same cell directly. This process effectively combines measurements from both radars at each sampling moment, increasing the number of jointly processed frames within the same sliding window duration. As a result, targets can be more effectively distinguished from noise.

Simulation results shown in Fig. 6 demonstrate a significant performance enhancement of the AT-MS-TBD compared to the traditional TBD algorithm employed with a single radar, especially under conditions of very low SNR.

3) Scenario 3

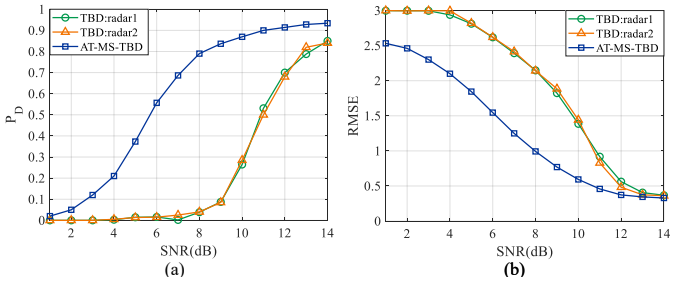

Fig. 6. Scenario 2: The Pd and RMSE curves of a single radar and the multi-radar system are plotted against target SNR.

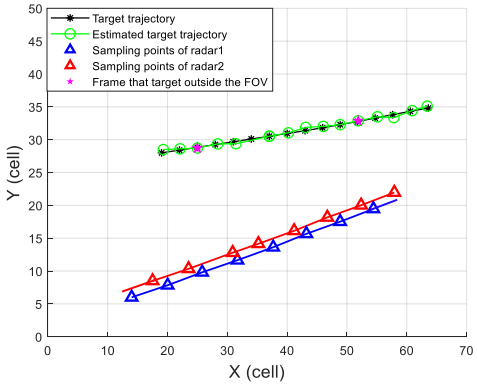

Fig. 7. Schematic diagram and the trajectory prediction results of the simulation scenario 3.

To enhance the illustration of the proposed method's scenario generalization, we devise a more complex and motorized scenario: two automotive radars may collect measurements and transfer them to the fusion center at any given moment, and the target temporarily exits the measurement area during the 3-th and 5-th frames. As shown in Fig. 7, the simulation scenario and the corresponding estimated results are exhibited. It can be seen that the AT-MS-TBD method can provide precise trajectory estimation, even when the target does not fall into the radar measurement area.

In summary, the proposed AT-MS-TBD method can fully utilize the measurements from different radars to accumulate target energy, thereby improving the estimation accuracy of weak targets.

VI. Conclusions

In this paper, we consider the target detection problem with multi-sensor TBD. The proposed AT-MS-TBD algorithm effectively solves the problem of target presence inconsistency in the sliding window, in which not only the movement of multi-radar platforms but also the limited field of view is taken into account. It could adaptively set the detection threshold based on the accumulation of target energy. Simulation results verified that the AT-MS-TBD can successfully track the target in both synchronized and asynchronous situations, and the proposed methods has a higher accuracy and robustness.

References

[1] D. Zhang, Z. Duan, and U. D. Hanebeck, "Asynchronous multi-radar tracking fusion with converted measurements," in *2022 25th International Conference on Information Fusion (FUSION)*. IEEE, 2022, pp. 1–8.

[2] Z. Wang, Y. Wu, and Q. Niu, "Multi-sensor fusion in automated driving: A survey," *Ieee Access*, vol. 8, pp. 2847–2868, 2019.

[3] X. R. Li, Y. Zhu, J. Wang, and C. Han, "Optimal linear estimation fusion. i. unified fusion rules," *IEEE Transactions on Information Theory*, vol. 49, no. 9, pp. 2192–2208, 2003.

[4] Y. Wang and X. R. Li, "Distributed estimation fusion with unavailable cross-correlation," *IEEE Transactions on Aerospace and Electronic Systems*, vol. 48, no. 1, pp. 259–278, 2012.

[5] F. Ehlers, D. Orlando, and G. Ricci, "Batch tracking algorithm for multistatic sonars," *IET Radar, Sonar & Navigation*, vol. 6, no. 8, pp. 746–752, 2012.

[6] G. Zhai, C. Wu, and Y. Wang, "Millimeter wave radar target tracking based on adaptive kalman filter," in *2018 IEEE Intelligent Vehicles Symposium (IV)*, 2018, pp. 453–458.

[7] E. Grossi, L. Venturino, and M. Lops, "A two-step multi-frame detection procedure for radar systems," in *2012 15th International Conference on Information Fusion*. IEEE, 2012, pp. 1196–1201.

[8] S. Buzzi, M. Lops, and L. Venturino, "Track-before-detect procedures for early detection of moving target from airborne radars," *IEEE Transactions on Aerospace and electronic systems*, vol. 41, no. 3, pp. 937–954, 2005.

[9] Z. Wang and J. Sun, "Maneuvering target tracking via dynamic-programming based track-before-detect algorithm," in *2016 CIE International Conference on Radar (RADAR)*. IEEE, 2016, pp. 1–4.

[10] L. Wang, G. Zhou, and T. Kirubarajan, "Track-before-detect technique in mixed coordinates," in *2018 21st International Conference on Information Fusion (FUSION)*. IEEE, 2018, pp. 1–6.

[11] N. Ito and S. Godsill, "A multi-target track-before-detect particle filter using superpositional data in non-gaussian noise," *IEEE Signal Processing Letters*, pp. 1075–1079, 2020.

[12] L. Wang, G. Zhou, and T. Kirubarajan, "Track-before-detect technique in mixed coordinates," in *2018 21st International Conference on Information Fusion (FUSION)*. IEEE, 2018, pp. 1–6.

[13] Y. Guo, Z. Zeng, and S. Zhao, "An amplitude association dynamic programming tbd algorithm with multistatic radar," in *2016 35th Chinese Control Conference (CCC)*. IEEE, 2016, pp. 5076–5079.

[14] W. Yi, Z. Fang, W. Li, R. Hoseinnezhad, and L. Kong, "Multi-frame track-before-detect algorithm for maneuvering target tracking," *IEEE Transactions on Vehicular Technology*, vol. 69, no. 4, pp. 4104–4118, 2020.

[15] J. Nidamanuri, C. Nibhanupudi, R. Assfalg, and H. Venkataraman, "A progressive review: Emerging technologies for adas driven solutions," *IEEE Transactions on Intelligent Vehicles*, vol. 7, no. 2, pp. 326–341, 2021.

[16] J. Wang, W. Yi, and L. Kong, "Multi-sensor dp-tbd based on approximation of likelihood functions," in *2017 20th International Conference on Information Fusion (Fusion)*, 2017, pp. 1–6.

[17] F. Ku, W. Yi, M. Wen, J. Wang, S. Li, and L. Kong, "Dynamic programming based track-before-detect methods for airborne radar system," in *2019 IEEE Radar Conference (RadarConf)*. IEEE, 2019, pp. 1–6.

[18] Y. Boers and P. K. Mandal, "Optimal particle-filter-based detector," *IEEE Signal Processing Letters*, vol. 26, no. 3, pp. 435–439, 2019.

[19] Z. Fang, W. Yi, G. Cui, L. Kong, R. Liu, and J. Yang, "A fast implementation of dynamic programming based track-before-detect for radar system," in *2015 IEEE Radar Conference (RadarCon)*. IEEE, 2015, pp. 0577–0580.

[20] J. Wang, W. Yi, L. Kong, and S. Guo, "Multi-frame detection method for distributed radar network," in *2018 IEEE Radar Conference (RadarConf18)*, 2018, pp. 0880–0884.

[21] J. Wang, W. Yi, R. Hoseinnezhad, and L. Kong, "An agile multi-frame detection method for targets with time-varying existence," *Signal Processing*, vol. 165, pp. 133–143, 2019.